

Emergence of Scenario-Appropriate Collaborative Behaviors for Teams of Robotic Bodyguards

Hassam Ullah Sheikh and Ladislau Bölöni

Department of Computer Science

University of Central Florida United States

hassam.sheikh@knights.ucf.edu, lboloni@cs.ucf.edu

Abstract

We are considering the problem of controlling a team of robotic bodyguards protecting a VIP from physical assault in the presence of neutral and/or adversarial bystanders. This task is part of a much larger class of problems involving coordinated robot behavior in the presence of humans. This problem is challenging due to the large number of active entities with different agendas, the need of cooperation between the robots as well as the requirement to take into consideration criteria such as social norms and unobtrusiveness in addition to the main goal of VIP safety. Furthermore, different settings such as street, public space or red carpet require very different behavior from the robot.

We describe how a multi-agent reinforcement learning approach can evolve behavior policies for teams of robot bodyguards that compare well with hand-engineered approaches. Furthermore, we show that an algorithm inspired by universal value function approximators can learn policies that exhibit appropriate, distinct behavior in environments with different requirements.

1 Introduction

Recent progress in the field of autonomous robots makes it feasible for robots to interact with multiple humans in public spaces. In this paper, we are considering a practical problem where a human VIP moving in various crowded scenarios is protected from physical assault by a team of bodyguard robots. This problem has been previously explored in (Bhatia et al. 2016) where explicitly programmed behaviors of robots were used to carry out the task.

Recent research in deep reinforcement and imitation learning has led to wide range of accomplishments in learning optimal policies for sequential decision making problems. These accomplishments include training agents in simulated environments such as playing Atari games (Mnih et al. 2015), beating the best players in board games like Go and Chess (Silver et al. 2016) as well as learning to solve real world problems.

With the recent advancements in the single agent Deep RL, there has been a renewed interest in multi-agent reinforcement learning (MARL) (Shoham, Powers, and Grenager 2007; Busoniu, Babuska, and De Schutter 2008). In MARL, there are several agents that interact with the environment to learn simultaneously either cooperatively,

competitively or a mixture of both. The goal of these agents is to either maximize their own utility individually or work in a team to maximize the utility of the group (Leibo et al. 2017; Tampuu et al. 2017).

MARL in its simplest form is known as independent RL (InRL), where each agent is oblivious to the other agents in the environment. InRL agents treat the interactions of other agents as a part of their local environment, which makes them non-stationary and non-Markovian (Laurent et al. 2011). This problem presents stability challenges for the learning agents and prohibit a straightforward use of the experience replay buffer which is a crucial step for learning any value function based method such as Q-learning or critic in policy gradient methods (Lowe et al. 2017).

Despite having outstanding performance in multiplayer games like Dota 2 (OpenAI 2018) and Quake III Capture-the-Flag (Jaderberg et al. 2018), MARL algorithms have failed to learn policies that can work in dynamic environments or have multiple goals (Cruz and Yu 2014). The multi-goal problem for single agent has been previously explored in (Schaul et al. 2015; Andrychowicz et al. 2017) where a universal value function approximator has been trained for a discrete set of goals.

Providing physical protection to a VIP through robot bodyguards is a complex task where the robots must take into account the position and movement of the VIP, the bystanders and other robots. The variety of environments and scenarios in which the bodyguards need to act presents another challenge. A possible way to solve this problem would be to use the expertise and training techniques of human bodyguards and program them into the robots. Unfortunately, these techniques are not documented in a formalizable language. Anecdotal evidence also points to human bodyguards using personal judgments about the movement, actions, body posture and facial expressions of different members of the crowd which are beyond the current capabilities of computer vision.

We aim to solve the VIP protection problem through multi-agent deep reinforcement learning while simultaneously learning to communicate and coordinate between the robots. We propose a novel general purpose technique that allows multi-agent learners to learn distributed policies not only over the state space but also over a set of different goals or scenarios. We show that our solution outperforms

a custom designed behavior, the quadrant load balancing method (Bhatia et al. 2016). As our formulation of the VIP protection problem is based on generic objective function, the approach can be generalized to other problems involving interactions between humans and mobile robots.

2 Background

We model the team of bodyguard robots as agents in a cooperative Markov game. Let \mathcal{S} be the set of states describing the possible configurations of agents, while \mathcal{A} the action space of all agents where \mathcal{A}_i is the action space of agent i . \mathcal{O} represents the observation space of all the agents where \mathcal{O}_i is the observation space of agent i . The behavior of agent i is described by policy $\pi_{\theta_i}(o_i)$ that outputs a distribution over actions a . An agent i performing action a in state s obtains a reward $r_i = R_i(s, a)$.

The return \mathcal{R}_i^t from state s at timestep t is defined as the discounted cumulative reward that the agent accumulates starting from state s at timestep t and represented as

$$\mathcal{R}_i^t = \sum_{t=0}^T \gamma^t r_i^t \text{ where } \gamma \text{ is the discount factor } \gamma \in [0, 1].$$

The goal of every agent is to find an optimum policy π^* that maximizes the expected return starting from state s .

2.1 Policy Gradients

Policy gradient methods have been shown to learn the optimal policy in a variety of reinforcement learning tasks. The main idea behind policy gradient methods is instead of parameterizing the Q-function to extract the policy, we parameterize the policy using the parameters θ to maximize the objective represented as $J(\theta) = \mathbb{E}[\mathcal{R}^t]$ by taking a step in the direction

$$\nabla J(\theta) = \mathbb{E}[\nabla_{\theta} \log \pi_{\theta}(a|s) Q^{\pi}(s, a)]$$

Policy gradient methods are prone to high variance problem. Several different methods such as (Wu et al. 2018; Schulman et al. 2017) have been shown to reduce the variability in policy gradient methods by introducing a critic which is a Q-function that tells about the goodness of a reward by working as a baseline.

(Silver et al. 2014) has shown that it is possible to extend the policy gradient framework to deterministic policies *i.e.* $\pi_{\theta} : \mathcal{S} \rightarrow \mathcal{A}$. In particular we can write $\nabla J(\theta)$ as

$$\nabla J(\theta) = \mathbb{E}[\nabla_{\theta} \pi(a|s) \nabla_a Q^{\pi}(s, a) |_{a=\pi(s)}]$$

A variation of this model, Deep Deterministic Policy Gradients (DDPG) (Lillicrap et al. 2015) is an off-policy algorithm that approximates the policy π and the critic Q^{π} with deep neural networks. DDPG also uses an experience replay buffer alongside a target network to stabilize the training.

Multi-agent deep deterministic policy gradients (MADDPG) (Lowe et al. 2017) extends DDPG for the multi-agent setting where each agent has its own policy. The gradient of each policy is written as

$$\nabla J(\theta_i) = \mathbb{E}[\nabla_{\theta_i} \pi_i(a_i|o_i) \nabla_{a_i} Q_i^{\pi}(s, a_1, \dots, a_N) |_{a_i=\pi_i(o_i)}]$$

where $s = (o_1, \dots, o_N)$ and $Q_i^{\pi}(s, a_1, \dots, a_N)$ is a centralized action-value function that takes the actions of all the

agents in addition to the state of the environment to estimate the Q-value for agent i . Since every agent has its own Q-function, the model allows the agents to have different action space and reward functions. The primary motivation behind MADDPG is that knowing all the actions of other agents makes the environment stationary, even though their policy changes.

The Universal Value Function Approximator (Schaul et al. 2015) is an extension of DQN (Mnih et al. 2015) for situations where there is more than one goal to achieve. Let \mathcal{G} be the set of all the goals and r_g be the reward function that corresponds to that particular goal. At the beginning of the episode, a state-goal pair is sampled from a probability distribution, the goal remains constant throughout the episode. At each timestep, the agent receives a pair of current state and goal and gets the reward $r^t = r_g(s^t, a^t)$. As a result, the Q-function is not only dependent on state-action pair but also on the goal. The extension of this approach is straight forward for DDPG (Andrychowicz et al. 2017) and MADDPG.

3 The VIP Protection Problem

We are considering a VIP moving in a crowd of bystanders $\mathcal{B} = \{b_1, b_2, \dots, b_m\}$ protected from assault by a team of robot bodyguards $\mathcal{R} = \{r_1, r_2, \dots, r_n\}$. To be able to reason about this problem, we need to quantify the *threat* to the VIP at a given moment - the aim of the bodyguards is to reduce this value.

We will use the threat model defined in (Bhatia et al. 2016). Two agents x and y have a *line of sight* $LoS(x, y) \in [0, 1]$ if x can directly observe y and with no obstacle between them. A bystander b can only pose a threat to the VIP if it is closer than the safe distance SafeDist . The *threat level* $TL(VIP, b)$ is defined as the probability that a bystander b can successfully assault the VIP, defined as a value exponentially decaying with distance:

$$TL(VIP, b) = \exp^{-A(\text{Dist}(VIP, b))/B} \quad (1)$$

where the VIP should be in line of sight of b and $\text{Dist}(VIP, b) < \text{SafeDist}$. A and B are positive constants that control the decay rate of the threat level.

The residual threat $RT(VIP, \mathcal{B}, R)$ is defined as the threat to the VIP at time t from bystanders \mathcal{B} . Bodyguards can block the line of sight from the bystanders, thus the residual threat is always smaller than the threat level and depends on the position of the bodyguards with respect to the bystanders and the VIP. The *cumulative residual threat* to the VIP from bystanders \mathcal{B} in the presence of bodyguards R over the time period $[0, T]$ is defined as:

$$\text{CRT} = \int_0^T 1 - \prod_{i=1}^k (1 - RT(VIP, b_i, R)) dt \quad (2)$$

Our end goal is to minimize CRT through multi-agent reinforcement learning.

3.1 Multi-Agent Universal Policy Gradient

Up to this point, we talked about a single bodyguard “behavior”. In practice the bodyguard needs to protect the VIP

under a variety of scenarios: indoors, outdoors, in a crowded mall, in a near-empty park, on the red carpet and so on. The behavior of the bodyguards must be different in these scenarios, and they must interpret bystander behavior differently. For instance, an unknown person coming towards the VIP needs to be interpreted differently on a narrow sidewalk, in a public plaza or on the red carpet. Experimental data (see Section 4.2) confirm that naïve MARL scenarios trained on specific environments perform poorly in different environments. In these situations the robotic bodyguard must make decisions that depend on factors that are not explicitly represented in the current observations that contain geometrical data about the VIP, team mates and bystanders.

To solve this problem, we propose to model these *scenarios* as different *goals*, in a multi-agent, multi-goal model. While generalization across multiple goals had been previously studied (Caruana 1997; Sutton et al. 2011; Schaul et al. 2015; Andrychowicz et al. 2017), to our best knowledge we are the first one to consider the multi-agent, multi-goal deep RL system.

Our approach uses Universal Value Function Approximators (Schaul et al. 2015) to train policies and value functions that take a state-goal pair as input. The outcome is a universal multi-agent policy that are able to perform on multiple goals as compared to policies that are trained separately.

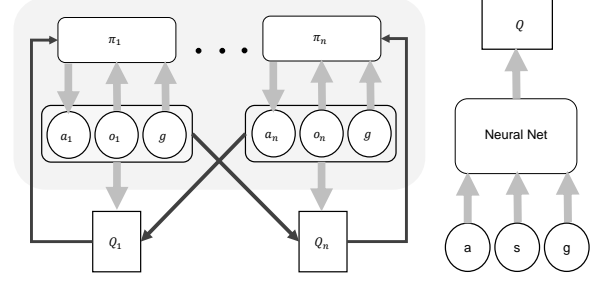
The main idea is to represent the different value function approximators for each agent i by single unified value function approximator that generalizes over both state space and the goals. For agent i we consider $V_i(s, g; \phi) \approx V_{i_g}^*(s)$ or $Q_i(s, a, g; \phi) \approx Q_{i_g}^*(s, a)$ that approximate the optimal unified value functions over multiple goals and a large state space. These value functions can be used to extract policies implicitly or as critics for policy gradient methods.

The training model we use is similar to the centralized training with decentralized execution during testing used by (Lowe et al. 2017). In this setting, additional information is provided for the agents during training that is not available during test time. Thus, extracting policies from value functions is not feasible in this model. However, the value functions can be used as critics in a multi-agent deep deterministic policy gradient setting.

Concretely, consider an environment with N agents with policies $\pi = \{\pi_1, \dots, \pi_N\}$ parameterized by $\theta = \{\theta_1, \dots, \theta_N\}$ then the *multi-agent deep deterministic policy gradient* for agent i can be written as

$$\nabla J(\theta_i) = \mathbb{E} [\nabla_{\theta_i} \pi_i(a_i | o_i) \nabla_{a_i} Q_i^\pi(s, a_1, \dots, a_N) |_{a_i = \pi_i(o_i)}]$$

where $s = (o_1, \dots, o_N)$ and $Q_i^\pi(s, a_1, \dots, a_N)$ is a centralized action-value function that takes the actions of all the agents in addition to the state of the environment to estimate the Q-value for agent i . We extend the idea of MADDPG with universal functional approximator, specifically we augment the centralized critic with goal. Now the modified pol-



(a) An overview of the multi-agent de- (b) Representation of centralized actor with centralized critic the single centralized represented by a universal value function approximator.

Figure 1: An overview of the multi-agent universal policy gradient architecture where both actors and critics are augmented with the goal that the agents are trying to achieve.

icy gradient for each agent i can be written as

$$\nabla J(\theta_i) = \mathbb{E}_{s, a \sim \mathcal{D}} \left[\nabla_{\theta_i} \pi_i(a_i | o_i | g) \nabla_{a_i} Q_i^\pi(s, a_1, \dots, a_N, g) \right] \quad (3)$$

where $a_i = \pi_i(o_i | g)$ is action from agent i following policy π_i and \mathcal{D} is the experience replay buffer. The centralized critic is Q_i^π is updated as:

$$\mathcal{L}(\phi_i) = \mathbb{E}_{s, a, r, s', g} [(Q_i^\pi(s, a_1, \dots, a_N, g)) - y]$$

where y is defined as:

$$y = r_i^g + \gamma Q_{\phi_i'}^{\pi'}(s', a'_1, \dots, a'_N, g) |_{a'_i = \pi'_i(o'_i | g)}$$

where $\pi' = \{\pi'_1, \dots, \pi'_N\}$ are target policies parameterized by $\theta' = \{\theta'_1, \dots, \theta'_N\}$.

The overall algorithm to which we refer as *multi-agent universal policy gradient* is described in Algorithm 1. The overview of the architecture can be seen in figure 1.

4 Experiments

This section is organized as follows. In section 4.1 we introduce the scenarios and reward function for the VIP protection problem as well as training details for our experiment. In section 4.2 we show that multi-agent reinforcement learning solution is better than quadrant load balancing technique introduced (Bhatia et al. 2016). In section 4.3 we compare our results of our technique with policies trained on scenarios individually. In section 4.4 we compare different ways of sampling scenarios.

4.1 Environments

As we discussed before, robotic bodyguards need to operate in different environments, exhibiting behavior appropriate to the specific threats that might appear in those environments.

Algorithm 1 Multi-agent Universal Policy Gradient

```
1: Sample a random scenario  $g$ 
2: for episode = 1 to  $M$  do
3:   for  $t = 1$  to episode-length do
4:     For each agent  $i$ , select action  $a_i^t = \pi_{\theta_i}(o_i^t \| g)$ 
5:     Execute actions  $\mathbf{a}_t = [a_1^t, \dots, a_N^t]$ 
6:     For each agent  $i$ , get next observation  $o_i^{t+1}$ 
7:   end for
8:   Sample an additional scenario  $k$ 
9:   for  $t = 1$  to episode-length do
10:    for agent  $i = 1$  to  $N$  do
11:      Get reward  $r_i^t := r_i^g(o_i^t, a_i^t)$ 
12:      Store  $(o_i^t, a_i^t, r_i^t, o_i^{t+1}, g)$  in replay buffer
13:      Get reward  $r_i^k := r_i^k(o_i^t, a_i^t)$ 
14:      Store  $(o_i^t, a_i^t, r_i^t, o_i^{t+1}, k)$  in replay buffer
15:    end for
16:  end for
17:  Set  $g = k$ 
18:  for agent  $i = 1$  to  $N$  do
19:    Sample minibatch of size  $S$   $(\mathbf{s}^j, \mathbf{a}^j, \mathbf{r}^j, \mathbf{s}'^j, \mathbf{g}^j)$ 
20:     $\mathbf{w} := (\pi_{\theta_i}^j(o_i^j \| g^j), \dots, \pi_{\theta_N}^j(o_N^j \| g^j))$ 
21:     $(a'_1, \dots, a'_N) := \mathbf{w}$ 
22:    Set  $y^j = r_i^j + \gamma Q_{\phi_i}^{\pi'}(\mathbf{s}'^j, a'_1, \dots, a'_N, \mathbf{g}^j)$ 
23:    Update critic by minimizing
      
$$\frac{1}{S} \sum_j (y^j - Q_{\phi_i}^{\pi'}(\mathbf{s}^j, a_1^j, \dots, a_N^j, \mathbf{g}^j))$$

24:    Update actor using equation (3)
25:  end for
26:  Update target network parameters for each agent  $i$ 
      
$$\theta'_i \leftarrow \tau \theta_i + (1 - \tau) \theta'_i$$

      
$$\phi'_i \leftarrow \tau \phi_i + (1 - \tau) \phi'_i$$

27: end for
```

To investigate the ability of the proposed multi-agent universal policy gradient algorithm to adapt to the different scenarios, we designed four scenarios inspired from possible real world situations of VIP protection and implemented them as behaviors in the Multi-Agent Particle Environment (Mordatch and Abbeel 2017) (Figure 2).

In each scenario, the participants are the VIP, four robot bodyguards and one or more classes of bystanders. The scenario description contains a number of *landmarks*, points on a 2D space that serve as starting point and destinations for the goal-directed movement by the agents. For each scenario, the VIP (brown disk) starts from the starting point and moves towards the destination landmark (green disk). The VIP exhibits a simple path following behavior, augmented with a simple social skill metric: it is about to enter the personal space of a bystander, it will slow down or come to a halt. The bodyguard robots are controlled by their own policies. Policies are represented as neural networks trained us-

ing algorithm described in Algorithm 1.

The scenarios differ in the number and arrangement of the landmarks and the behavior of the different classes of bystanders.

- **Random Landmark:** In this scenario, landmarks are placed randomly in the area. The starting point and destination for the VIP are randomly selected landmarks. The bystanders are performing random waypoint navigation: they pick a random landmark, move towards it, and when they reached it, they choose a new destination.
- **Shopping Mall:** In this scenario, landmarks are placed in fixed position on the periphery of the area, representing shops in a market. The bystanders visit randomly selected shops.
- **Street:** This scenario aims to model the movement on a crowded sidewalk. The bystanders are moving towards waypoints that are outside the current area. However, due to their proximity to each other, the position of the other bystanders influence their movement described by laws of particles motion (Vicsek et al. 1995).
- **Pie-in-the-Face:** While the in other scenarios the bystanders treat the VIP as just another person, in this “red carpet” scenario the bystanders take an active interest in the VIP. We consider two distinct classes of bystanders with different behaviors. *Rule-abiding* bystanders stay behind a designated line observing as the VIP passes in front of them. *Unruly* bystanders break the limit imposed by the line and try to approach the VIP (presumably, to throw a pie in his/her face).

The state of the environment is given by $s = [o_1, \dots, o_{N+M}, c_1, \dots, c_N] \in \mathcal{S}$. The observation of each agent is the physical state of all the entities in the environment and verbal utterances of all the agents $o_i = [x_j, \dots, x_{N+M}, c_k, \dots, c_N] \in \mathcal{O}_i$ where x_j is the observation of the entity j from the perspective of agent i and c_k is the verbal utterance of the agent k .

Reward Functions

In (Bhatia et al. 2016) has defined a metric that quantifies the threat to the VIP from each crowd member b_i at each timestep t . This metric can be extended to a reward function. Since the threat level metric gives a probability. We can conclude that when the distance between the VIP and the crowd member is 0, the threat to the VIP is maximum, i.e 1, conversely when the distance between the VIP and the crowd member b_i is more than the *safe distance*, the threat to the VIP is 0. We can model this phenomenon as an exponential decay. In the following we will derive reward function and explain the motivation behind them that were derived from equation 2.

The baseline *Threat-Only Reward Function* penalizes each agent with the threat to the VIP at each time step as mentioned in (Bhatia et al. 2016).

$$r_g = -1 + \prod_{i=1}^k (1 - RT(VIP, b_i, R)) \quad (4)$$

The *Composite Reward Function* is the composition of the threat only reward function and the penalty for not maintaining a suitable distance from the VIP.

$$\mathcal{D}(VIP, x_i) = \begin{cases} 0 & m \leq \|x_i - VIP\|_2 \leq d \\ -1 & \text{otherwise} \end{cases} \quad (5)$$

where m is the minimum distance the bodyguard has to maintain from VIP and d is the safe distance. The final reward function is represented as

$$r_g = \alpha \left(-1 + \prod_{i=1}^k (1 - RT(VIP, b_i, R)) \right) + \beta (\mathcal{D}(VIP, x_i)) \quad (6)$$

Each scenario g has different values of α, β and m , thus fulfilling the requirement of different goals having different reward structure.

In this problem, we are assuming that all bodyguards have observation space and they are following an identical policy. For this problem we are considering a finite horizon problem where each episode is terminated after T steps. Since this problem is a cooperative setting, the goal of all the agents is to find individual policies that increase the collected payoff.

4.2 Multi-Agent Reinforcement Learning vs Quadrant Load Balancing

In order to verify that multi-agent reinforcement learning solutions are better than explicitly programmed behavior of the bodyguards, we evaluate policies trained on individual scenarios with quadrant load balancing technique introduced in (Bhatia et al. 2016).

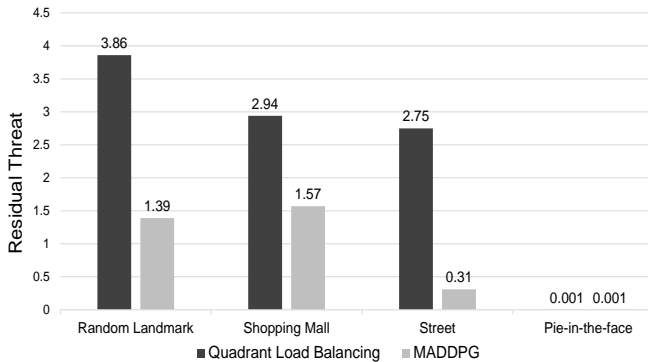


Figure 3: Comparing the average residual threat values for agents trained using the multi-agent deep deterministic policy gradient versus agents implementing the QLB algorithm in different scenarios over 100 episodes.

The multi-agent reinforcement learning experiments were performed by training bodyguards using multi-agent deep deterministic policy gradient (Lowe et al. 2017) in Multi-Agent Particle Environment (Mordatch and Abbeel

2017). The experiments were performed with four bodyguards and the number of bystanders were kept constant ten bystanders. The performance of both methods was measured using the residual threat metric (Bhatia et al. 2016). Training details can be found in section 5.

From the results in Figure 3 we can see that the results are different depending on the characteristics of the scenario. For the Pie-in-the-face scenario, where most of the bystanders stay away behind the lines, both the RL-learned agent and the QLB model succeeded to essentially eliminate the threat. This was feasible in this specific setting, as there were four bodyguard agents for one “unruly” bystander. For the other scenarios, the residual threat values are higher for both algorithms. However, for the Random Landmark and Shopping Mall scenarios the RL algorithm is able to reduce the threat to less than half, while in the case of the Street scenario, to less than one ninth of the QLB value.

Overall, these experiments demonstrate that the multi-agent reinforcement learning can learn behaviors that improve upon algorithms that were hand-crafted for this specific task.

4.3 Universal Policy Vs Scenario-Dependant Policy

In order to verify the claim that MARL algorithms trained on specific scenario fail to generalize over different scenarios, we evaluate policies trained via MADDPG on specific scenario and test them on different scenarios. Policies on specific scenarios were trained using the same settings and configurations from experiments performed in section 4.2.

	RL	SM	Street	Pie-in-the-Face
RL	1.39	1.80	0.39	0.02
SM	3.49	1.57	0.40	0.03
Street	2.77	2.00	0.31	0.16
Pie-in-the-Face	3.96	3.24	2.64	0.001

Table 1: A correlation matrix representing the average residual threat values of MADDPG policies trained on specific scenario when tested on different scenarios over 100 episodes. The row represents the training scenario and the column represents the testing scenario.

From the results shown in Table 1 we can see that MADDPG policies trained on specific scenarios performed poorly when tested on different scenarios as compared to when tested on same scenario with different seeds. In order to tackle the generalization problem, we train the agents using multi-agent universal policy gradient and compare with the results of scenario-dependant MADDPG policies.

From the results in Figure 4 we can see that our proposed method performs better than policies trained on specific scenarios. Overall, these experiments demonstrate that the proposed model can learn behaviors that improve upon the start-of-the-art multi-agent reinforcement learning algorithm.

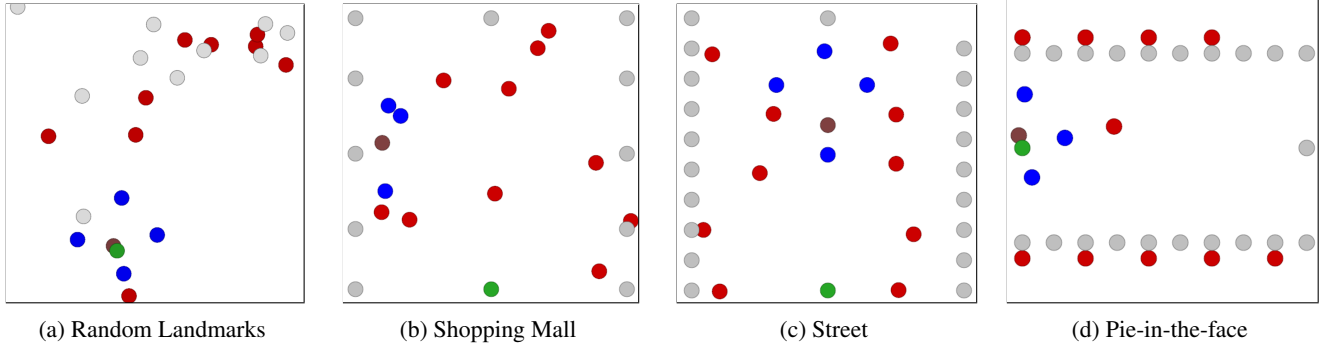


Figure 2: Visual representation of the four different scenarios. Emergence of complex behavior can be clearly seen in 2a, 2b and 2d where the bodyguards (in blue) have positioned themselves between the VIP (in brown) and the bystanders (in red) shielding from potential threat.

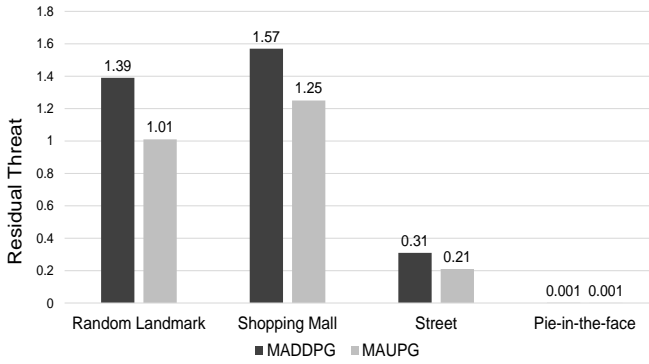


Figure 4: Comparing the average residual threat values for agents trained using the multi-agent universal policy gradient (universal policy) versus agents trained using multi-agent deep deterministic policy gradient (scenario-dependant policies) in different scenarios over 100 episodes.

For sake of completeness, the comparison between performance of all three methods can be seen in Figure 5.

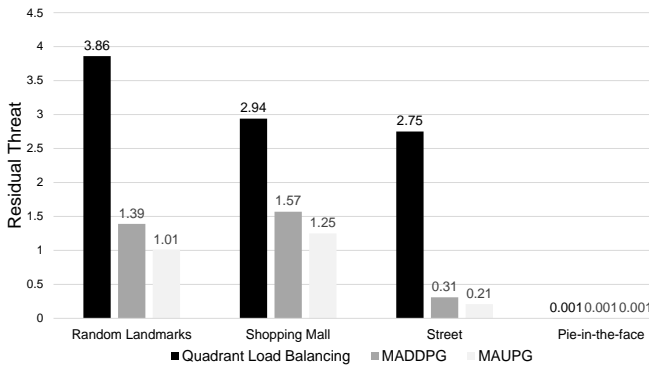


Figure 5: Comparing the residual threat values for universal policy agents when the environments were sampled randomly versus when environments were sampled using softmax trick.

4.4 Sampling Strategy

In this section, we experimentally evaluate results of two sampling strategies to sample the environment. The two strategies we compared are

- Random uniform sampling
- Softmax sampling

Different scenarios have different levels of threat i.e some scenarios pose a higher threat to the VIP as compared to other scenarios. In our case, shopping mall scenario is more difficult to train as compared to pie-in-the-face as the later scenario has only one moving bystander thus the shopping mall scenario needs to be sampled more than the pie-in-the-face scenario. For this purpose, we used softmax for sampling environments.

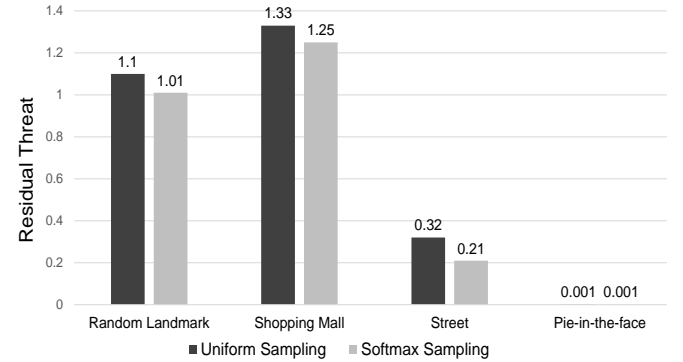


Figure 6: Comparing the average residual threat values for universal policy agents when the environments were sampled randomly versus when environments were sampled using softmax trick.

Let P_k be $\frac{\sum_i^n CRT/n}{\sum_i^n CT/n}$ that represents the performance of the policy on environment k over n previous episode that also normalizes performance across scenarios. Higher value of P_k represents worst performance. At the end of each episode we calculate $\mathbf{P} = (P_1, \dots, P_m)$ where m represents number of scenarios. \mathbf{P} is fed to a softmax that converts the

performance of policy on scenarios into probability distribution and an environment is sampled from the probability distribution.

From the results in Figure 6, we can see that sampling scenarios through softmax outperforms uniform random sampling and can achieve an improvement of more than 10% over uniform random sampling.

5 Experimental Details

In this section we provide the details of the experimental setup along with the hyperparameters that were used.

5.1 Environment Model

For performing the experiments, we built our environments in Multi-Agent Particle Environment (Mordatch and Abbeel 2017). MPE is a two-dimensional physically simulated environment in a discrete time and continuous space. Our environment consists of N agents and M landmarks, both possessing physical attributes such as location, velocity and size etc.

In addition to providing physical attributes, the MPE environment also allows agents to communicate with each other over a communication channel at every timestamp. At each timestamp, every agent utters a categorical variable that is observed by every other agent and it is up to the agents to infer a meaning of these symbols during the training time. Every utterance carry a small penalty. This penalty discourages agents to communicate at every timestamp since human bodyguards do not communicate at every timestamp. The utterance from each agent is represent as a vector \mathbf{c} .

5.2 Simulations

The Random Landmark scenario consists of 12 landmarks that were randomly placed in the environment. A set of fixed seeds were used for placement of landmarks and a different set of seeds were used for spawning bystanders in the environment and were moving towards randomly selected shops.

The Shopping Mall scenario consists of 12 landmarks that represent shops in a shopping mall that were placed on fixed positions. The bystanders were spawned using a fixed set of random seeds and were moving towards randomly selected shops.

The Street scenario consists of 22 landmarks that were placed on fixed positions. The bystanders were spawned on fixed positions. The movement of the bystanders follows the Vicsek model for particle motion (Vicsek et al. 1995).

The Pie-in-the-Face scenario consists of 22 landmarks that were placed on fixed positions. All the bystanders are stationary except a randomly chosen bystander as an attacker that tries to attack the VIP.

All the scenarios have 2 fixed landmarks that are used as starting and destination point for the VIP except in the case of Random Landmark scenario where starting and destination points were also chosen randomly.

Network Architecture

Both actor and critic networks for all agents consists of 2 hidden layers containing 64 units in each layer. The hidden

layers uses ReLU activation function while the output layers of both networks use linear activation function. Both networks are initialized using random weights but the output layer of the critics were initialized with zero weights to enable one-step learning of the critics after each training cycle. Same architecture was used across all the experiments.

Training Procedure

Policies for each environment were trained using different set of parameters while keeping the length of each episode 25 across all experiments. Random Landmark scenario was trained for 10,000 episodes. The other 3 remaining environments were trained for 8000, 8000 and 6000 episodes respectively. The universal was trained for 15000 episodes. Minibatches of size 1024 were sampled from replay buffer of size 10^7 for each agent and 4 optimization steps were performed on all the critics. We update the target network after every optimization cycle using Polyak Averaging with decay coefficient of 0.99. For Adam optimization algorithm we used learning rate of 0.003 and default values from TensorFlow framework (Abadi et al. 2015) for remaining hyperparameters. Finally for training the universal we used the discount factor of 0.85 and used values of 0.95, 0.9, 0.7 and 0.8 for training strategies for Random Landmark, Shopping mall, Street and Pie-in-the-Face scenarios respectively.

Exploration

The behavior policy for every agent works as follows. The actor network takes the state as an input and outputs an action. A noise is added to each dimension of the action using a stochastic process i.e Ornstein–Uhlenbeck process.

6 Conclusions and Future Work

In this paper, we have first formulated the problem of providing maximal protection to a VIP through robotic bodyguards into a feasible multi-agent deep reinforcement learning problem. Given this setting, we first presented MADDPG based solution outperforms the quadrant load balancing technique. We highlighted the problem of generalization that multi-agent reinforcement learning algorithms face across various goals. To solve the generalization problem, we proposed *multi-agent universal policy gradient*, a universal value function approximator inspired policy gradient method that not only generalizes over state space but also over set of different goals. Experimental studies on VIP protection problem have demonstrated that our proposed method generalizes well on different scenario and performs better than MADDPG when trained on different scenarios individually.

In this paper, we tried to solve a human-robot interaction problem through multi-agent reinforcement learning where a multi-robot system is interacting with human beings in real world scenarios. This opens many research questions such as building bodyguard teams with a combination of humans and robots. On the other hand, a formal investigation of multi-agent universal policy gradient has been left for future work.

References

- [Abadi et al. 2015] Abadi, M.; Agarwal, A.; Barham, P.; Brevdo, E.; Chen, Z.; Citro, C.; Corrado, G. S.; Davis, A.; Dean, J.; Devin, M.; Ghemawat, S.; Goodfellow, I.; Harp, A.; Irving, G.; Isard, M.; Jia, Y.; Jozefowicz, R.; Kaiser, L.; Kudlur, M.; Levenberg, J.; Mané, D.; Monga, R.; Moore, S.; Murray, D.; Olah, C.; Schuster, M.; Shlens, J.; Steiner, B.; Sutskever, I.; Talwar, K.; Tucker, P.; Vanhoucke, V.; Vasudevan, V.; Viégas, F.; Vinyals, O.; Warden, P.; Wattenberg, M.; Wicke, M.; Yu, Y.; and Zheng, X. 2015. TensorFlow: Large-scale machine learning on heterogeneous systems. Software available from tensorflow.org.
- [Andrychowicz et al. 2017] Andrychowicz, M.; Wolski, F.; Ray, A.; Schneider, J.; Fong, R.; Welinder, P.; McGrew, B.; Tobin, J.; Pieter Abbeel, O.; and Zaremba, W. 2017. Hind-sight experience replay. In *Advances in Neural Information Processing Systems 30*, 5048–5058.
- [Bhatia et al. 2016] Bhatia, T.; Solmaz, G.; Turgut, D.; and Bölöni, L. 2016. Controlling the movement of robotic bodyguards for maximal physical protection. In *Proc. of the 29th International FLAIRS Conference*, 380–385.
- [Busoniu, Babuska, and De Schutter 2008] Busoniu, L.; Babuska, R.; and De Schutter, B. 2008. A comprehensive survey of multiagent reinforcement learning. *IEEE Trans. on Systems, Man and Cybernetics Part C* 38(2):156–172.
- [Caruana 1997] Caruana, R. 1997. Multitask learning. *Machine Learning* 28(1):41–75.
- [Cruz and Yu 2014] Cruz, D. L., and Yu, W. 2014. Multi-agent path planning in unknown environment with reinforcement learning and neural network. In *IEEE Int’l Conf. on Systems, Man, and Cybernetics (SMC)*, 3458–3463.
- [Jaderberg et al. 2018] Jaderberg, M.; Czarnecki, W. M.; Dunning, I.; Marris, L.; Lever, G.; Castaneda, A. G.; Beattie, C.; Rabinowitz, N. C.; Morcos, A. S.; Ruderman, A.; Sonnerat, N.; Green, T.; Deason, L.; Leibo, J. Z.; Silver, D.; Hassabis, D.; Kavukcuoglu, K.; and Graepel, T. 2018. Human-level performance in first-person multiplayer games with population-based deep reinforcement learning. *arXiv preprint arXiv: 1807.01281*.
- [Laurent et al. 2011] Laurent, G. J.; Matignon, L.; Fort-Piat, L.; et al. 2011. The world of independent learners is not markovian. *International Journal of Knowledge-based and Intelligent Engineering Systems* 15(1):55–64.
- [Leibo et al. 2017] Leibo, J. Z.; Zambaldi, V.; Lanctot, M.; Marecki, J.; and Graepel, T. 2017. Multi-agent reinforcement learning in sequential social dilemmas. In *Proc. of the 16th Int’l Conf. on Autonomous Agents and Multiagent Systems (AAMAS)*, 464–473.
- [Lillicrap et al. 2015] Lillicrap, T. P.; Hunt, J. J.; Pritzel, A.; Heess, N.; Erez, T.; Tassa, Y.; Silver, D.; and Wierstra, D. 2015. Continuous control with deep reinforcement learning. In *Proc. of the 3rd Int’l Conf. on Learning Representations (ICLR)*.
- [Lowe et al. 2017] Lowe, R.; Wu, Y.; Tamar, A.; Harb, J.; Abbeel, P.; and Mordatch, I. 2017. Multi-agent actor-critic for mixed cooperative-competitive environments. In *Advances in Neural Information Processing Systems 30*, 6379–6390.
- [Mnih et al. 2015] Mnih, V.; Kavukcuoglu, K.; Silver, D.; Rusu, A. A.; Veness, J.; Bellemare, M. G.; Graves, A.; Riedmiller, M.; Fidjeland, A. K.; Ostrovski, G.; Petersen, S.; Beattie, C.; Sadik, A.; Antonoglou, I.; King, H.; Kumaran, D.; Wierstra, D.; Legg, S.; and Hassabis, D. 2015. Human-level control through deep reinforcement learning. *Nature* 518(7540):529–533.
- [Mordatch and Abbeel 2017] Mordatch, I., and Abbeel, P. 2017. Emergence of grounded compositional language in multi-agent populations. *arXiv preprint arXiv:1703.04908*.
- [OpenAI 2018] OpenAI. 2018. *OpenAI Five*. <https://blog.openai.com/openai-five/>.
- [Schaul et al. 2015] Schaul, T.; Horgan, D.; Gregor, K.; and Silver, D. 2015. Universal value function approximators. In *Proc. of the 32nd Int’l Conf. on Machine Learning (ICML)*, 1312–1320.
- [Schulman et al. 2017] Schulman, J.; Wolski, F.; Dhariwal, P.; Radford, A.; and Klimov, O. 2017. Proximal policy optimization algorithms. *arXiv preprint arXiv:1707.06347*.
- [Shoham, Powers, and Grenager 2007] Shoham, Y.; Powers, R.; and Grenager, T. 2007. If multi-agent learning is the answer, what is the question? *Artificial Intelligence* 171(7):365–377.
- [Silver et al. 2014] Silver, D.; Lever, G.; Heess, N.; Degris, T.; Wierstra, D.; and Riedmiller, M. 2014. Deterministic policy gradient algorithms. In *Proc. of the 31st Int’l Conf. on Machine Learning (ICML)*, 387–395.
- [Silver et al. 2016] Silver, D.; Huang, A.; Maddison, C. J.; Guez, A.; Sifre, L.; van den Driessche, G.; Schrittwieser, J.; Antonoglou, I.; Panneershelvam, V.; Lanctot, M.; Dieleman, S.; Grewe, D.; Nham, J.; Kalchbrenner, N.; Sutskever, I.; Lillicrap, T.; Leach, M.; Kavukcuoglu, K.; Graepel, T.; and Hassabis, D. 2016. Mastering the game of Go with deep neural networks and tree search. *Nature* 529:484–503.
- [Sutton et al. 2011] Sutton, R. S.; Modayil, J.; Delp, M.; Degris, T.; Pilarski, P. M.; White, A.; and Precup, D. 2011. Horde: A scalable real-time architecture for learning knowledge from unsupervised sensorimotor interaction. In *Proc. of the 10th Int’l Conf. on Autonomous Agents and Multiagent Systems (AAMAS)*, 761–768.
- [Tampuu et al. 2017] Tampuu, A.; Matiisen, T.; Kodelja, D.; Kuzovkin, I.; Korjus, K.; Aru, J.; Aru, J.; and Vicente, R. 2017. Multiagent cooperation and competition with deep reinforcement learning. *PloS one* 12(4):e0172395.
- [Vicsek et al. 1995] Vicsek, T.; Czirók, A.; Ben-Jacob, E.; Cohen, I.; and Shochet, O. 1995. Novel type of phase transition in a system of self-driven particles. *Physical review letters* 75(6):1226.
- [Wu et al. 2018] Wu, C.; Rajeswaran, A.; Duan, Y.; Kumar, V.; Bayen, A. M.; Kakade, S.; Mordatch, I.; and Abbeel, P. 2018. Variance reduction for policy gradient with action-dependent factorized baselines. In *Proc. of the 6th Int’l Conf. on Learning Representations (ICLR)*.